https://doi.org/10.5194/bg-2023-4
Preprint. Discussion started: 19 January 2023
© Author(s) 2023. CC BY 4.0 License.

Biogeosciences Discussions

Spatial and temporal variability of methane emissions and environmental conditions in a hyper-eutrophic fishpond

Petr Znachor[1,2], Jiří Nedoma[1], Vojtech Kolar[1, 3], Anna Matoušů[1]

[1]Biology Centre of Czech Academy of Sciences, v.v.i., Institute of Hydrobiology, Na Sádkách 7, České Budějovice, 37005, Czech Republic

[2]Faculty of Science, University of South Bohemia, Branišovská 1760, České Budějovice, 37005, Czech Republic

[3]Biology Centre of Czech Academy of Sciences, Institute of Entomology, Branišovská 31, České Budějovice, 370 05, Czech Republic

*Correspondence to:*Anna Matoušů (anna.matousu@gmail.com)

Abstract. Estimations of methane (CH_4) emissions are often based on point measurements using either flux chambers or a transfer coefficient method which may lead to strong underestimation of the total CH_4 fluxes. In order to demonstrate more precise measurements of the CH_4 fluxes from an aquaculture pond, using higher resolution sampling approach we examined the spatiotemporal variability of CH_4 concentration in the water, related fluxes (diffusive and ebullitive) and relevant environmental conditions (temperature, oxygen, chlorophyll-a) during three diurnal campaigns in a hyper-eutrophic fishpond. Our data show remarkable variance spanning several orders of magnitude while diffusive fluxes accounted for only a minor fraction of total CH_4 fluxes (4.1–18.5 %). Linear mixed-effects models identified water depth as the only significant predictor of CH_4 fluxes. Our findings necessitate complex sampling strategies involving temporal and spatial variability for reliable estimates of the role of fishponds in a global methane budget.

Keywords: aquaculture, emissions, fishpond, freshwater, heterogeneity, methane

https://doi.org/10.5194/bg-2023-4
Preprint. Discussion started: 19 January 2023
© Author(s) 2023. CC BY 4.0 License.

Biogeosciences Discussions

1 Introduction

Freshwater aquaculture ponds (fishponds) represent man-made counterparts to natural shallow lakes (Scheffer, 2004) which are mainly used for fish production (mostly of common carp, *Cyprinus carpio* L.) and water retention in the landscape. Fishponds serve also as secondary biotope for various organisms (Kolar et al., 2021), supporting noteworthy animal and plant diversity (Pokorný and Hauser, 2002). However, most fishponds suffer from high fish stock densities, excessive carbon and nutrient loading from supplemental fish feeding, sewage pollution, and fertiliser runoffs from agricultural catchments or nutrient mobilisation from the anoxic sediment layers (Pechar, 2000). As a result, the trophic structure of plankton communities has shifted towards a reduction of large zooplankton and massive development of phytoplankton, especially cyanobacterial blooms (Potužák et al., 2007), limiting light penetration in the water column. Rapid changes in the intensity of biological processes such as photosynthesis and respiration often result in pronounced daily or seasonal fluctuations in dissolved oxygen (Baxa et al., 2021), signalling decreasing ecosystem stability. The extent of anoxia, accumulation of organic biomass, and rapid heating of the shallow water during summer result in enhanced production of greenhouse gases (Grasset et al., 2018, Zhang et al., 2021; Bartosiewicz et al., 2021).

Most concerning are CH_4 emissions as freshwater aquaculture systems release more than 6 Tg CH_4 yr^{-1} (Yuan et al., 2019). Methane can be emitted via several pathways: simple molecular diffusion, ebullition (in the form of bubbles released from oversaturated sediments), plant-mediated flux (Bastviken et al., 2004), but also through so far neglected pathways including aeration, emissions from dry/drying sediments, or dredged organic material (Kosten et al., 2020). Among all, ebullition is considered the dominant pathway (van Bergen et al., 2019; Kosten et al., 2020), which can contribute 50-96 % (Casper et al., 2000; Xiao et al., 2017; van Bergen et al., 2019; Yang et al., 2020; Zhao et al., 2021) to the total CH_4 flux. Along with the second important pathway – molecular diffusion, both exhibit high spatiotemporal variability due to various physical and biological factors acting on very short time scales, for instance, temperature (van Bergen et al., 2019), eutrophication (Zhang et al., 2021), water depth (DelSontro et al., 2016), CH_4 production rates (Zhou et al., 2019), CH_4 oxidation rates (Sanseverino et al., 2013), dissolved oxygen concentration (Xiao et al., 2017), management regime (Yang et al., 2019), or the quality of organic matter in the sediment (Schmiedeskamp et al., 2021). Recently, the direct involvement of phytoplankton in CH_4 production and emissions has been emphasised (Yan et al., 2019; Bižić et al., 2020; Bartosiewicz et al., 2021).

https://doi.org/10.5194/bg-2023-4
Preprint. Discussion started: 19 January 2023
© Author(s) 2023. CC BY 4.0 License.


Although fishponds are recognised as powerful model systems for studies in ecology and evolutionary or conservation biology (De Meester et al., 2005; Céréghino et al., 2008), the extent of environmental heterogeneity in fishponds and shallow Inland small waterbodies remains poorly understood (Ortiz and Wilkinson, 2021), largely because the driving factors are either system-specific or highly variable on short time scales (Laas et al., 2012). Most of current information on lentic ecosystem structure and function comes from single-site sampling, in which measurements are taken over time at the deepest point in the lake, which does not sufficiently account for within-lake spatial variation (Stanley et al., 2019). The motivation for our study was the growing concern about the role of fishponds as important sources of CH_4 fluxes to the atmosphere (Wik et al., 2016). Unfortunately, the majority of global CH_4 flux estimates rely on upscaling methods (DelSontro et al., 2018a) based on a limited number of measurements that do not account for diurnal and seasonal variability or ecosystem spatial heterogeneity. Yang et al. (2019) indicates that a larger number of spatial replicates over a number of months is mandatory to improve the accuracy of whole-pond CH_4 flux estimates. The published research from other aquaculture studies have been performed mainly in tropical and subtropical zones in fish or crab aquacultures (e.g., Hu et al., 2016; Ma et al., 2018; Yang et al., 2019, 2020; Yuan et al., 2019, 2021). To better understand the spatial dynamics of CH_4 fluxes and environmental heterogeneity in temperate freshwater shallow lake, we conducted a spatial sampling of the hyper-eutrophic Dehtář fishpond (Czech Republic, Europe). Since the seasonal CH_4 production is strongly affected by temperature, we focused on warm summer months where the total CH_4 fluxes were expected to be the highest (Jansen et al., 2020). The objectives of our study were (i) to determine the spatial heterogeneity of CH_4 diffusive and total fluxes and fundamental limnological variables (oxygen, temperature, chlorophyll-a) and they change daily and monthly in the hyper-eutrophic pond, and (ii) to identify the factors that influence CH_4 fluxes to improve our understanding of the importance of spatiotemporal variability for global estimates of CH_4 efflux to the atmosphere.

2 Material and Methods

2.1 Study site description

The Dehtář fishpond (49° N, 14° E) is a shallow man-made lake (average and maximum depth: 2.4 and 6 m) constructed in 1479 and used for polycultural, semi-intensive production of common carp (Potužák et al., 2016). It lies in a flat agricultural landscape at 406.4 m above sea level in the upper Vltava River basin in South Bohemia (Czech Republic) which is characteristic with its network of fishponds (Fig. 1b). Due to the orography of the

https://doi.org/10.5194/bg-2023-4
Preprint. Discussion started: 19 January 2023
© Author(s) 2023. CC BY 4.0 License.

landscape, the Dehtář fishpond, surrounded by narrow belts of littoral vegetation and adjacent to grassland and arable land, is exposed to wind, mainly from the northwest (for aerial photograph, see Suppl. Fig 1). The catchment area is 91.4 km^2. The main inflow is the Dehtářský stream in the south, while several smaller tributaries flow in from the west (Fig. 1c). The fishpond has a dam 234 m long and 10 m high, with two outlets and a safety spillway. Covering 2.28 km^2, the Dehtář fishpond is among the ten largest fishponds in the Czech Republic, holding a volume of 4.71 × 10^3 m^3 and having a water residence time of 146-445 days (Potužák et al., 2016).

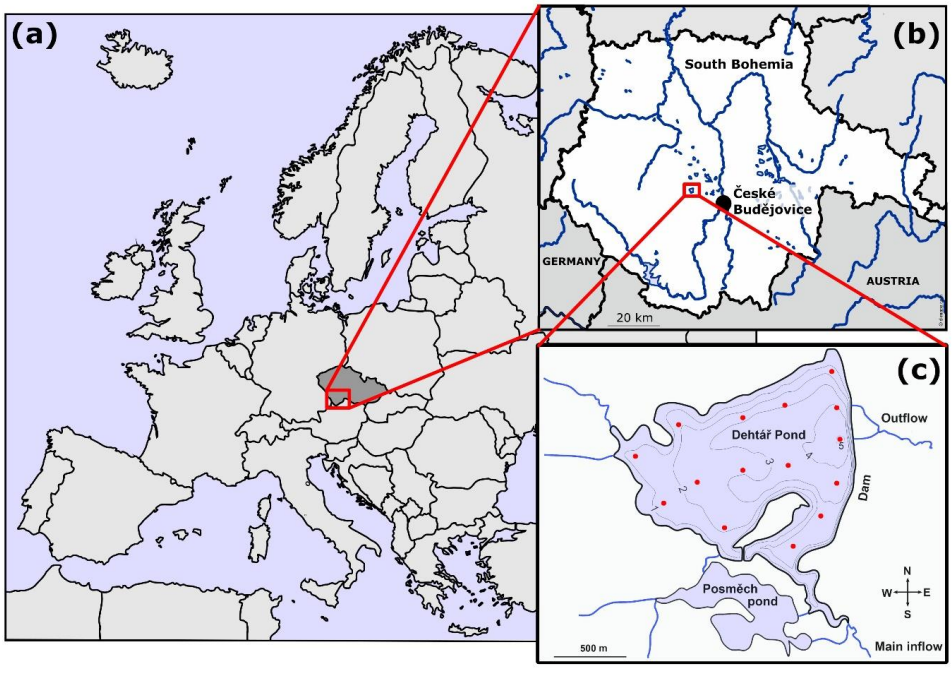

Figure 1. Location (a, b; copyright www.d-maps.com; https://d-maps.com/carte.php?num_car=2232&lang=en and https://d-maps.com/carte.php?num_car=265046&lang=en; modified) and bathymetric map (c; credit Jiří Jarošík) of the sampled Dehtář fishpond: Blue lines indicate hydrological connections; red dots are the sampling points. Numbers indicate isobath depth.

2.2 Sampling design and measurement

To measure spatial heterogeneity and temporal changes in limnological parameters and methane fluxes, we conducted three 36-hour surveys in summer 2019 (July 2-3, August 13-14, September 19-20). In the morning (between 5-6 a.m.), we first measured surface values and vertical profiles of temperature, oxygen, and chlorophyll-*a* concentration at the deepest point (see below for details). We subsequently installed 15 floating polyethylene gas chambers (as shown in Fig. 1c), serving as fixed sampling sites and at the same time for accumulation of CH_4 fluxes (see further), starting in the western part of the fishpond. During installation (and further during each

https://doi.org/10.5194/bg-2023-4
Preprint. Discussion started: 19 January 2023
© Author(s) 2023. CC BY 4.0 License.


sampling), temperature, pH, and oxygen concentration were measured at 0.3 m depth using the WTW 330i pH meter and Oximeter (WTW, Weilheim, Germany). Vertical chlorophyll-*a* profiles were measured at each sampling site using a submersible fluorescence probe (FluoroProbe, bbe-Moldaenke, Kiehl, Germany). From each site, the average chlorophyll-*a* concentration in the surface layer (0-1 m depth) was used to assess the phytoplankton spatial heterogeneity.

To minimise the chance that the differences observed among sites were due to time of day, we conducted repeated measurements at the deepest point at the end of each sampling. If there was a change, all values were corrected for the sampling time by linear interpolation:

$$P_{corr} = P_t + (P_{end} - P_0) \times \frac{(t-t_0)}{(t_{end}-t_0)} \quad (1)$$

where P_{corr} is the corrected value of a parameter, P_t is its value measured at the time t, P_0 and P_{end} are parameter values measured at the deepest point at the start (time t_0) and at the end (t_{end}) of the sampling. In the evening and morning of the second day (roughly at 12 h intervals), we performed additional measurements of spatial heterogeneity, allowing us to assess diurnal and nocturnal changes. In addition, samples for measuring CH_4 concentration in the surface water were collected at each site and analysed as described below. To assess diurnal variations in thermal structure and oxygen concentration in the water column, we made vertical profile measurements at the deepest point at 3-6 h intervals using the YSI EXO 2 multiparametric probe (YSI Inc., Yellow Springs, USA).

2.3 Methane measurements

Water samples for determining CH_4 concentration in the surface water were collected at all 15 sampling sites in triplicates into 20 ml glass bottles. The bottles were capped bubble-free under water with black butyl rubber stoppers (Ochs, Germany) and sealed with aluminium crimps. Immediately after sampling, the water samples were preserved by injecting 100 µl of concentrated sulfuric acid to stop the microbial activity (Bussmann et al., 2015). The samples were processed within one week in the laboratory using a headspace technique according to McAuliffe (1971). Methane concentration in the headspace was measured using an HP 5890 Series II gas chromatograph (Agilent Technologies, USA) and calculated with the solubility coefficient given by Yamamoto et al. (1976).

Methane diffusive fluxes (F) were then calculated for each sampling site indirectly using the 2-layer model with the equation:

$$F = k\left(C_{sur} - C_{eq}\right) \quad (2)$$

https://doi.org/10.5194/bg-2023-4
Preprint. Discussion started: 19 January 2023
© Author(s) 2023. CC BY 4.0 License.

where C_{sur} is the CH_4 concentration in surface water in μmol L^{-1}, C_{eq} is the CH_4 concentration in surface water in equilibrium with the atmosphere in μmol L^{-1}, and k is the CH_4 exchange constant (cm h^{-1}). The value of k was calculated from the local wind speed according to Crusius and Wanninkhof (2003):

$$k = k_{600}\left(\frac{Sc}{600}\right)^{n} \quad (3)$$

where k_{600} is the gas transfer velocity for a Schmidt number (Sc) of 600. The Schmidt number for CH_4 was calculated according to Wanninkhof (2014):

$$Sc = 1909.4 - 120.78t + 4.1555t^2 - 0.080578t^3 + 0.000658t^4 \quad (4)$$

where t (°C) is the water temperature at the time of CH_4 extraction. The parameter C_{eq} in Eq. (1) was determined from the equation:

$$C_{eq} = \beta \times pCH_4 \quad (5)$$

where β is the solubility coefficient of CH_4 as a function of temperature according to Wiesenburg and Guinasso (1979), and pCH_4 is the partial pressure of CH_4 in the atmosphere.

To estimate total CH_4 fluxes from the water column to the atmosphere (i.e., diffusive and ebullitive fluxes), we measured CH_4 accumulation in open-bottom floating polyethylene chambers (volume 3.1 L; area 0.024 m^2). Each gas chamber was anchored at individual 15 fixed sampling sites, but allowed to float freely on the water surface. Gas was accumulating for approximately 12 h during each sampling period, i.e., during the day and night periods. Afterwards, 30 ml of gas was carefully taken from each chamber, after mixing the headspace in the chamber, and stored in evacuated Exetainers® (Labco Limited, UK). Chambers were ventilated after each sampling period to reset the incubation conditions. Methane fluxes were calculated as the difference between initial background and final concentration in the chamber headspace and expressed on the 1 m^2 area of the surface level per day according to Bastviken et al. (2004).

2.4 Background limnological parameters

During each campaign, samples for analysis of nutrient concentration and phytoplankton composition were collected from the surface at the deepest point using a Friedinger sampler. Water transparency was measured using a Secchi desk. Total phosphorus (TP) and soluble reactive phosphorus (SRP) were analysed spectrophotometrically according to Kopáček and Hejzlar (1993) and Murphy and Riley (1962), respectively. Concentrations of NH_4^+ and NO_3^- were determined according to the procedure of Kopáček and Procházková (1993) and Procházková (1959), respectively. Phytoplankton samples were preserved with Lugol's solution and

https://doi.org/10.5194/bg-2023-4
Preprint. Discussion started: 19 January 2023
© Author(s) 2023. CC BY 4.0 License.


examined for species composition with an inverted microscope (Olympus IMT-2). Weather data were obtained from the gauging station at the fishpond dam.

2.5 Statistical analyses

Two-tailed paired Student's t-tests and Two-way ANOVA with post-hoc Tukey's multiple comparison test (Prism 9.3, GraphPad Software Inc., La Jolla, USA) tested for differences between diffusive and total CH_4 fluxes between day and night and among three sampling campaigns, respectively. The percentage of data variability explained by different factors (daytime, month and site) was calculated with the Two-way RM ANOVA. Contour graphs illustrating changes in spatial heterogeneity of measured parameters were constructed in Surfer 10 (Golden Software, Inc., Colorado, USA) using the kriging contouring method. Spatial heterogeneity was quantified by calculating the spatial variance (i.e., coefficient of variation):

$$CV\% = 100 \times \frac{SD}{mean} \quad (6)$$

Higher spatial variance indicates increasing ecosystem patchiness. Linear mixed-effects models were used to analyse the effects of O_2, pH, temperature, and water depth on the CH_4 diffusive fluxes with the random effect of time of day nested within the effect of sampling date. The most parsimonious model was obtained by a manual backward selection, where we sequentially removed all insignificant predictors ($p > 0.05$) using likelihood ratio tests implemented in the drop1 function (Zuur et al., 2009). We also compared the slopes of the month-specific regression lines produced by the model using analysis of covariance (Zar, 1984). Linear mixed-effects models were implemented in the lme4 package version 1.1-21 (Bates et al., 2015), and Kenward-Roger F-tests were computed using the ANOVA Type II function from the pbkrtest package version 0.4-7 (Halekoh and Hojsgaard, 2014). The prediction of the resulting final model was visualised in the package ggeffects version 0.14.1 (Lüdecke, 2018). Package performance version 0.4.4 (Lüdecke et al., 2020) was used to calculate Nakagawa's R^2 of the linear model. The statistical analyses were performed using R software (v. 3.5.2, R Core Team, 2018).

3 Results

3.1 Weather and background fishpond characteristics

Weather parameters varied among sampling campaigns. In July, clear skies prevailed with the daily air temperature above 30 °C (Table 1). During the August and September measurements, it was very cloudy, and daily air temperatures decreased to 22 and 18 °C, respectively. The water level was stable during the whole studied period

https://doi.org/10.5194/bg-2023-4
Preprint. Discussion started: 19 January 2023
© Author(s) 2023. CC BY 4.0 License.

with a monthly fluctuation of ~ 10 cm. Water transparency was low (15-40 cm), with an increasing trend towards the end of summer (Table 1). Concentrations of total phosphorus and soluble reactive phosphorus were high (Table 1), consistent with a hyper-eutrophic state of the fishpond. In contrast, nitrogen concentrations were rather low, with ammonium nitrogen being the predominant form of inorganic N in the water (Table 1).

Table 1: Basic characteristics of the Dehtář fishpond during the studied period.

	July	**August**	**September**
Weather	Clear sky, windy	Partly cloudy, no wind	Partly cloudy, no wind
Air temperature (°C)	25-32	20-22	11-18
PHAR (mol m^{-2} day^{-1})	9.5	3.4	5.0
Secchi depth (cm)	15	30	40
TP (µg l^{-1})	568	527	406
SRP (µg l^{-1})	100	200	107
N-NH_4^+ (µg l^{-1})	23	783	560
N-NO_3^- (µg l^{-1})	14	23	46
Chl-*a* (µg l^{-1})	456	156	185
Phytoplankton composition	Cyanobacteria	Cyanobacteria, green algae, cryptophytes	Cryptophytes, green algae

Chlorophyll-*a* concentrations were highest in July due to the dense cyanobacterial bloom accumulated at the surface (Table 1). The phytoplankton consisted of only three cyanobacterial taxa: *Dolichospermum flos-aquae*, *Planktothrix agardhii*, and *Raphidiopsis mediteranea*. In August, phytoplankton was more diverse but also dominated by cyanobacteria: *P. agardhii*, *Aphanizomenon issatschenkoi*, and *D. flos-aquae*. In September, cyanobacteria were absent and instead, cryptophytes (*Cryptomonas reflexa*), green algae (*Pediastrum*, *Coelastrum* and *Desmodesmus*) and dinoflagellates (*Ceratium hirundinella*) prevailed.

3.2 Methane concetration and fluxes

The CH_4 concentration in surface water was highly supersaturated over the whole studied period. The obtained values varied from 0.003 up to 3.75 µmol L^{-1} (Fig. 2), which corresponded to saturation levels of 108-12 834%. It is obvious, that the obtained data show remarkable variance: the mean (± SD) values were 0.22 ± 0.18 for July, 0.34 ± 0.45 for August, and 1.61 ± 0.61 µmol L^{-1} for September (Suppl. Fig. 11).

https://doi.org/10.5194/bg-2023-4
Preprint. Discussion started: 19 January 2023
© Author(s) 2023. CC BY 4.0 License.

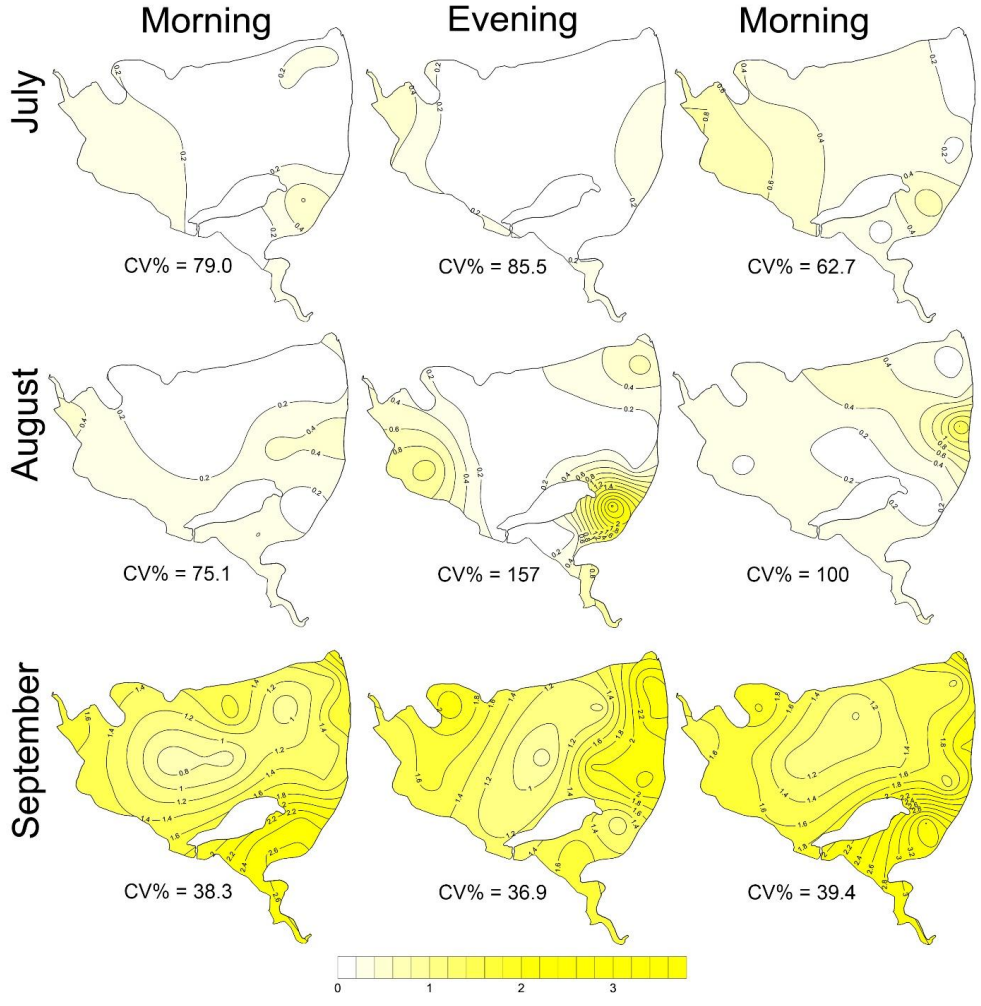

Figure 2: Contour graphs illustrating both seasonal and daily changes in spatial heterogeneity (indicated by the coefficient of variation, CV%) of the surface methane concentration (μmol L^{-1}) in the fishpond.

Diffusive fluxes (i.e., calculated from CH_4 concentration, see Eq. 2) showed the lowest values in July and August (average 0.12 and 0.16 mmol m^{-2} d^{-1}, respectively) and pronouncedly peaked in September (average 0.78 mmol m^{-2} d^{-1}, Fig. 3a). By contrast, in July and August, the average total CH_4 fluxes (obtained with floating chambers) showed the highest values (average 31.8 mmol m^{-2} d^{-1}; ranging from 0.08 to 152 mmol m^{-2} d^{-1}) while in September, total CH_4 fluxes were three times lower than before (average 11.8 mmol m^{-2} d^{-1}, range 0.3 to 43.5 mmol m^{-2} d^{-1}, Fig 3b). As a result, diffusive fluxes accounted for only a minor fraction of total CH_4 fluxes to the atmosphere (on average, 9.2 % in July, 4.1 % in August, 18.5 % in September, Fig. 3c).

https://doi.org/10.5194/bg-2023-4
Preprint. Discussion started: 19 January 2023
© Author(s) 2023. CC BY 4.0 License.

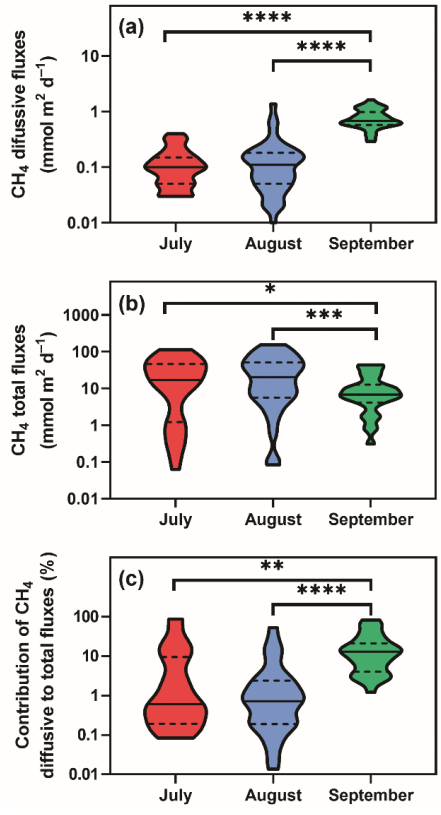

Figure 3: Violin plots of CH_4 diffusive (a) and total fluxes (b) during the studied period. Panel (c) depicts differences in the percentage contribution of diffusive to total fluxes. Solid lines are medians, while dashed lines denote quartiles. Asterisks indicate significant differences (* $p<0.05$, ** $p<0.01$, *** $p<0.001$, **** $p<0.0001$) between sampling dates determined by two-way ANOVA with Tukey's multiple comparison test. Note that a log scale is used here for clarity.

The total CH_4 fluxes show spatial variability within the fishpond that range several orders of magnitude (Fig. 3, 4; Suppl. Fig. 11; Suppl. Table 1). The observed spatial pattern showed high temporal variability on both daily and monthly scales (Fig. 2, 4, Suppl. Table 1). Most of the variability in CH_4 diffusive fluxes was explained by sampling date (62.4 %), while for the total CH_4 fluxes, spatial heterogeneity accounted for 87.2 % of data variability (Table 2). Using linear mixed-effects models, we identified water depth as the only significant predictor of total CH_4 fluxes ($Df = 1$, $p < 0.0001$, marginal Nakagawa's $R^2 = 0.348$; Fig. 5).

https://doi.org/10.5194/bg-2023-4
Preprint. Discussion started: 19 January 2023
© Author(s) 2023. CC BY 4.0 License.

Table 2: The percentage of data variability explained by different factors (daytime, month = sampling date, and site) calculated with the Two-way RM ANOVA. Statistical significant values ($p < 0.01$) are bold.

	% of variability				Significance		
	Daytime	**Month**	**Site**	**Unexplained**	**Daytime**	**Month**	**Site**
CH_4 diffusive flux	2.3	**62.4**	13.2	22.1	0.0123	<0.0001	*n.s.*
CH_4 total flux	0.19	2.4	**87.2**	10.2	*n.s.*	*n.s.*	<0.0001
pH	**4.4**	**64.9**	11.1	19.6	0.0001	<0.0001	*n.s.*
Water temperature	**3.3**	**92.3**	**2.5**	1.9	<0.0001	<0.0001	<0.0001
O_2	**21.7**	**48.1**	**13.8**	16.4	<0.0001	<0.0001	0.0135
Chl-*a*	0.019	**74.9**	**16.7**	8.4	*n.s.*	<0.0001	<0.0001

Interestingly, slopes of the linear regressions differed significantly among individual sampling campaigns (Fig. 5), indicating an additional season-related factor that affects CH_4 fluxes in the fishpond. Calculated CH_4 diffusive fluxes were not correlated with total fluxes. Linear mixed-effects models did not identify any significant predictor of the fluxes, indicating that factors and processes out of the study's scope are involved. We found no significant difference in either diffusive or total CH_4 fluxes between day and night.

https://doi.org/10.5194/bg-2023-4
Preprint. Discussion started: 19 January 2023
© Author(s) 2023. CC BY 4.0 License.

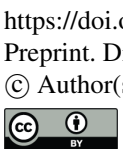

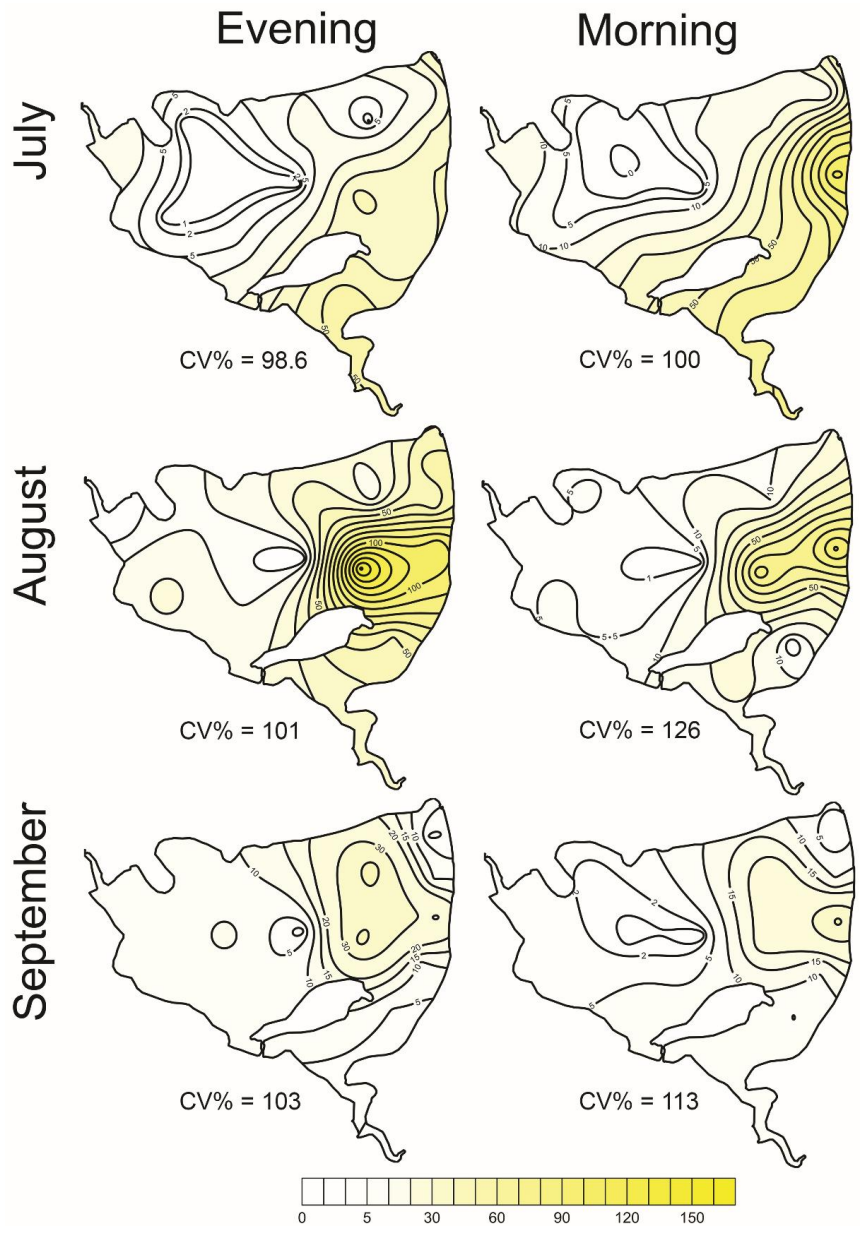

Figure 4: Contour graphs of methane total fluxes in the Dehtář fishpond. Isopleths connect sites with the same value of methane fluxes (mmol m^{-2} day^{-1}). CV% is a measure of spatial heterogeneity.

https://doi.org/10.5194/bg-2023-4
Preprint. Discussion started: 19 January 2023
© Author(s) 2023. CC BY 4.0 License.

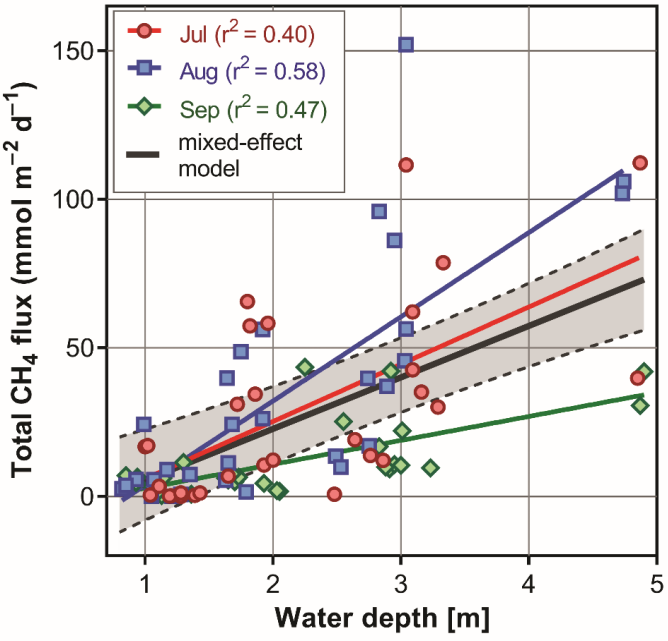

238

239 **Figure 5:** The most parsimonious linear mixed-effect model of methane total fluxes showing the water depth as the only
240 significant predictor. Symbols are the measured values, the solid black line is the prediction, and dashed lines are 95th
241 confidence intervals. Colours indicate month specific relation between total methane fluxes and water depth. Differences in
242 slopes were tested using the F-test. In September, the slope of the regression line was significantly different from that in July
243 and August.

244 **3.3 Diurnal changes in vertical profiles of oxygen and temperature**

245 Several contrasting patterns of vertical temperature and oxygen profiles occurred during summer 2019. Diurnal
246 changes were most pronounced in July (Fig. 6). Surface temperatures varied from 25 °C in the morning to nearly
247 30 °C in the afternoon. Thermal stratification of the water column was weak in the morning but became strongest
248 at 14:30 with a thermocline at 0.5 m depth (Fig. 6). Later in the afternoon, the water column began to be mixed by
249 wind. The morning vertical oxygen profile was characterised by a surface value of 4.3 mg L^{-1}, corresponding to
250 51 % saturation and anoxia below 3 m.

https://doi.org/10.5194/bg-2023-4
Preprint. Discussion started: 19 January 2023
© Author(s) 2023. CC BY 4.0 License.

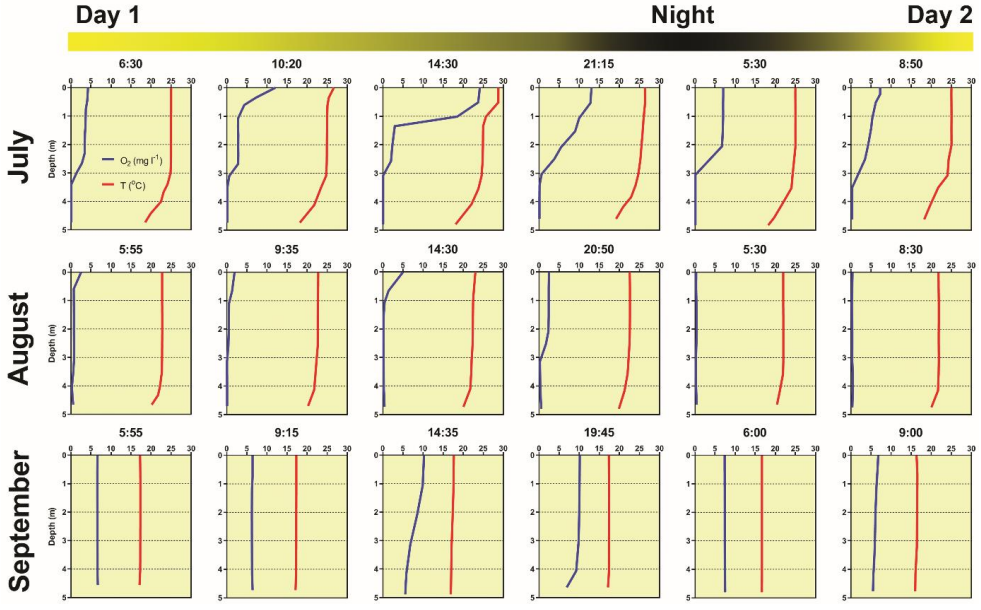

Figure 6: Diurnal changes in vertical profiles of temperature and oxygen concentration measured at the deepest point of the fishpond. Numbers above each graph indicate the time of measurement.

Due to the high photosynthetic activity of cyanobacteria, the surface oxygen concentration increased to 24 mg L^{-1} (320 % saturation, Fig. 6), and a steep oxycline was established at a depth of 0.5-1.5 m with no effect on the anoxic conditions at the deeper layers. Wind action eroded both the oxy- and thermoclines in the evening, and by the next morning, the vertical profiles were similar to those at the beginning.

In August, the water column was almost entirely mixed and low in oxygen in the morning, with only 2.6 mg L^{-1} (30 % saturation) of oxygen at the surface. Due to cloudy weather, the daily photosynthetic activity of phytoplankton resulted in only a slight increase in oxygen concentration at 0-1.5 m depth (4 mg L^{-1}, 47 % saturation). By the morning of the next day, the entire water column turned very close to anoxic (0.4 mg L^{-1}, 4 % saturation; Fig. 6), which in turn affected the spatial distribution of zooplankton, as evidenced by the formation of dense zooplankton clouds accumulated in the thin layer just at the surface (see Suppl. Fig. 3). In September, the water column was completely mixed, and we observed only weak daily changes in thermal and oxygen vertical structures (Fig. 6).

3.4 Effect of wind on spatial heterogeneity of temperature, oxygen and chlorophyll-*a*

During the summer, all measured parameters showed remarkable within-lake spatial heterogeneity (Suppl. Fig. 4-8). In July, meteorological conditions allowed for demonstrating the effect of wind on fishpond spatial

https://doi.org/10.5194/bg-2023-4
Preprint. Discussion started: 19 January 2023
© Author(s) 2023. CC BY 4.0 License.

heterogeneity. In the morning, there were no substantial differences in the surface temperature and oxygen concentrations (Fig. 7ab). Phytoplankton biomass was accumulated mostly in the shallow western part, with the maximum in the centre (Fig. 6c). At 14:00, a light breeze started to blow from the northwest, achieving a maximum of 11 km h^{-1} (Suppl. Fig. 7). This episode lasted till the evening measurement, and the wind ceased by 21:00. The wind was strong enough to change spatial distribution substantially (Fig. 7d-f, Suppl. Fig. 4). In the evening, the surface water temperature on the windward (south) side of the fishpond was ~ 4 °C higher than in the north (Fig. 7d). The wind also induced order of magnitude differences in oxygen concentration along the north-south axis of the fishpond (3 mg L^{-1} of O_2 at the north, 24 mg L^{-1} of O_2 at the south; Fig. 7e) and affected phytoplankton distribution in the fishpond, resulting in remarkable bloom accumulation in the south (Fig. 7f, Suppl. Fig. 8). During the calm night after the disturbance, the north-south gradient substantially weakened. In August and September, the thermal heterogeneity of the pond was rather low, but the spatial distribution of oxygen and chlorophyll-*a* remained highly variable (Suppl. Fig. 5–8, Suppl. Table 1).

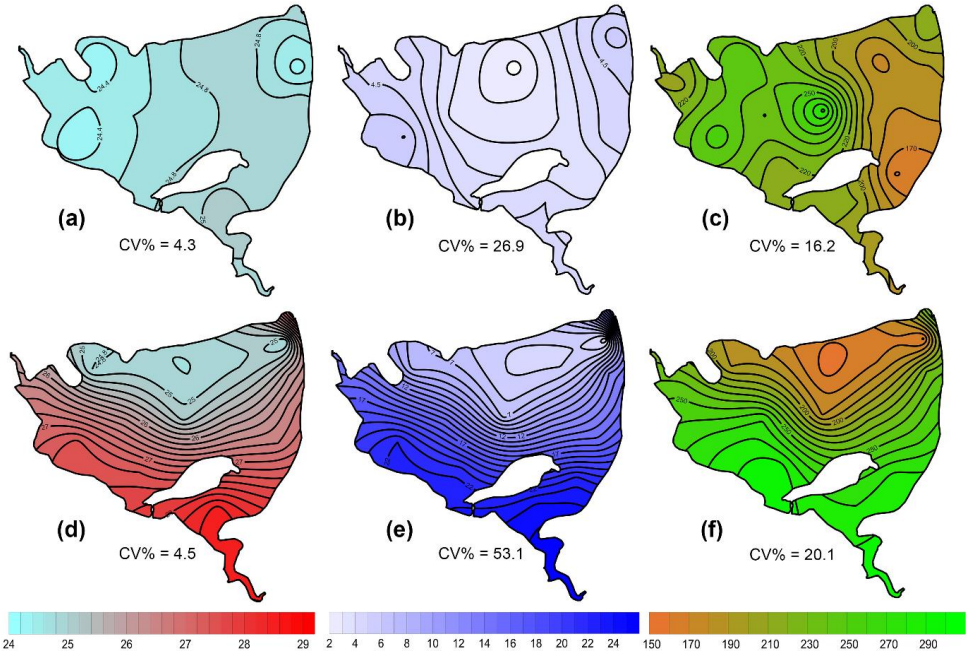

Figure 7: Contour graphs of surface temperature (a, d; °C), oxygen concentration (b, e; mg L^{-1}) and chlorophyll-a concentration (c, f; µg L^{-1}) measured on July 2 at different times of day: a, b and c are the morning measurements; d, e and f are evening measurements following a wind disturbance. Coefficient of variation (CV %) is a measure of spatial heterogeneity of measured parameters.

https://doi.org/10.5194/bg-2023-4
Preprint. Discussion started: 19 January 2023
© Author(s) 2023. CC BY 4.0 License.

Discussion

4.1 Methane fluxes

Assessing spatial heterogeneity of the CH_4 fluxes within a fishpond is critical for a reliable estimate of its contribution to the global CH_4 budget. In our study, the variability in total CH_4 fluxes spanned several orders of magnitude (ranging from 0.06 up to 1 121.3 mmol m^{-2} d^{-1}), which is in agreement with similar studies (Casper et al., 2000; DelSontro et al., 2016; Natchimutu et al., 2016). However, most system-specific CH_4 flux estimates rely on upscaling from a limited number of sites (Bastviken et al., 2004; Rasilo et al., 2015; Wik et al., 2016) because obtaining spatial variability in CH_4 emission is methodologically challenging. In general, spatial heterogeneity may reflect differences in water sources, physical mixing, local transformations and biogeochemical processes and rates among lake habitats (Loken et al., 2019). In deep lakes, littoral areas can contribute disproportionately to total lake CH_4 fluxes (Hofmann et al., 2010; Hofmann 2013, Natchimuthu et al., 2016; Schilder et al., 2013) and are often missed by traditional sampling approaches (Wik et al., 2016). According to Wik et al. (2016), low temporal and spatial resolutions are unlikely to cause overestimates. On the other hand, DelSontro et al. (2018b) suggested that horizontal transport of CH_4 produced in littoral zones and the interaction between physical and biological processes (e.g. air-water gas exchange, water column mixing, the interplay between CH_4 production and microbial oxidation) may result in an underestimation of whole-lake CH_4 fluxes based on centre samples. Similarly, Natchimuthu et al. (2016) found that up to 78 % underestimation would occur if samples obtained only from the lake center are used to extrapolate the total CH_4 flux. However, extrapolating our data from the deepest point of the Dehtář fishpond would lead to an overestimation of the CH_4 fluxes by a factor of 2.9 (Suppl. Fig. 12). The bias introduced by the deepest point measurement appears to be highly variable among systems with different morphology, geographical location, mixing regimes or trophic states. For instance, analysis of 22 European lakes during late summer has shown that spatially resolved CH_4 diffusive fluxes were highly variable for individual lakes, yielding 55–300 % differences in the whole-lake estimates (Schilder et al., 2013). Schmiedeskamp et al. (2021) observed an increase in CH_4 fluxes from the shore towards the centre in response to increasing sediment C-content in two shallow German lakes. In line with these findings, our results provide further evidence that spatially resolved data are needed to validate the uncertainties that come from using single-point samples to represent whole-lake processes in hyper-eutrophic systems. As stated by Loken et al. (2019), rather than assuming spatial homogeneity, scaling-up exercises of global carbon budgets should acknowledge the uncertainty that comes from extrapolating from spatially limited data sets.

https://doi.org/10.5194/bg-2023-4
Preprint. Discussion started: 19 January 2023
© Author(s) 2023. CC BY 4.0 License.

In the Dehtář fishpond, the total CH_4 fluxes increased with water depth, and this relationship was month specific. The highest CH_4 fluxes at the deepest points may seem contradictory to previous studies, in which the highest fluxes were typically observed in littoral areas (e.g. DelSontro et al., 2018b; Hofman et al., 2010; Natchimuthu et al., 2016; Schilder et al., 2013). However, these findings are based on studying mostly lakes whose morphology, trophic state or oxygen regime sharply contrast with the Dehtář fishpond, where the upper two meters of the water column were oxygen-saturated while the deepest strata were mostly anoxic. In such hyper-eutrophic systems, high nutrient loading increases autochthonous primary production (Potužák et al., 2007; Rutegwa et al., 2019) and promotes oxygen consumption and anaerobic decomposition in the sediments (Baxa et al., 2020), leading to enhanced CH_4 production (Bastviken et al., 2004; Grasset et al., 2018). In aquaculture ponds in Southeast China, CH_4 fluxes exhibited considerable spatial variations and peaked in the relatively deep feeding zone, where the large loads of sediment organic matter fueled CH_4 production (Yang et al., 2020). Furthermore, sediment temperature was the strongest predictor of CH_4 fluxes in ponds (DelSontro et al., 2016; Yang et al., 2020). It is, therefore, reasonable to assume that both temperature and oxygen concentration in the sediment likely contributed to changes in observed CH_4 fluxes during the studied period in our study. Although both parameters were not directly measured in the sediment, it can be deduced from their vertical profiles that the probability of sediment anoxia was highest in August and lowest in September, and the sediment temperature was lowest in September (see Fig. 5).

Our results agree with the generally accepted view that processes other than diffusive fluxes – most likely ebullition – represent the major CH_4 pathway to the atmosphere in hyper-eutrophic ponds (Kosten et al., 2020). Although freshwaters with high primary production are more likely to have high CH_4 ebullition rates (DelSontro et al., 2016), the dominant role of ebullition was also found across lentic systems differing in size, trophic status or geographical location (Aben et al., 2017). Ebullition accounted on average for 56 % of total CH_4 fluxes in northern ponds in Canada (DelSontro et al., 2016), 49 and 71 % in two different zones of Lake Taihu (Xiao et al., 2017) and 48-83 % in three Swedish lakes (Natchimuthu et al., 2016; Jansen et al., 2019). The highest contribution was found in the small hyper-eutrophic Priest Pot (UK), where ebullition represented 96 % of the total CH_4 flux from the pond (Casper et al., 2000). Apparently, the contribution of ebullition can vary among systems and will remain uncertain until measurement designs cover enough spatiotemporal variability to yield representative values for the whole ecosystem.

In shallow water bodies, a semi-stable flux of microbubbles was suggested to account for a significant portion of the total CH_4 flux (Prairie and del Giorgio, 2013). When CH_4 concentration in the water column is above a certain

https://doi.org/10.5194/bg-2023-4
Preprint. Discussion started: 19 January 2023
© Author(s) 2023. CC BY 4.0 License.


345 threshold of microbubble density, these microbubbles likely aggregate, fuse, and escape to the atmosphere from
346 buoyancy (Prairie and del Giorgio, 2013). Even a small fluctuation in hydrostatic pressure (e.g., due to changes in
347 atmospheric pressure) or lake water level was shown to trigger enhanced CH_4 ebullition (Bastviken et al., 2004;
348 Casper et al., 2000; Varadharajan and Hemond, 2012). Since ebullition rates increase exponentially with
349 temperature, CH_4 fluxes tend to peak in warm summer months (van Bergen et al., 2019). In our study, 1 % lower
350 air pressure in July and August than in September, along with bottom anoxia and higher water temperature, could
351 account for the enhanced release of CH_4 bubbles from the sediment (31.7 mmol $m^{-2}d^{-1}$, >90 % of total CH_4 fluxes;
352 Suppl. Fig. 2). In September, when we observed the lowest water temperatures from the studied period and the
353 oxygen profile was rather uniform, ebullition accounted for 81 % (11 mmol $m^{-2}d^{-1}$) of the total CH_4 fluxes. The
354 spatially pooled data of the total CH_4 fluxes measured in the Dehtář fishpond varied from 11.8 to 34.5 mmol m^{-2}
355 d^{-1}, which is comparable with similar systems elsewhere (e.g., Bastviken et al., 2010; van Bergen et al., 2019;
356 Baron et al., 2022). To sum up, both diffusive fluxes and ebullition must be addressed to understand the magnitude
357 of total aquatic CH_4 fluxes and how their relative contributions vary across and within aquatic systems (Kosten et
358 al., 2020). Moreover, with an improved determination of CH_4 hot-spots and its causes, the management of ponds
359 could be changed accordingly and so the overall emissions reduced for example by decreasing P-availability and
360 dredging (Nijman et al., 2022).

361 **4.2 Effect of wind event on ecosystem spatial structure**

362 Sudden changes in ecosystem spatial structure in response to meteorological forcing have rarely been documented
363 (Loken et al., 2019) since they are hard to predict. Research into them using traditional methods requires intensive
364 effort or expensive instrumentation (Ortiz and Wilkinson, 2021), and it remains a matter of luck to obtain a relevant
365 dataset. In the July sampling campaign, we observed a strong impact of the wind on environmental heterogeneity
366 in the fishpond, which was apparent at a sub-daily time scale. Due to the methodological constraints, i.e., lack of
367 initial measurement, we can only speculate about the effect of wind on the total CH_4 fluxes. The northwest wind
368 during the day advected warmed surface water with cyanobacterial bloom from the north basin to the south. In the
369 evening, it resulted in bloom accumulation on the upward side and a north-south gradient of more than 4 °C and
370 4-24 mg L^{-1} oxygen. After the winds fell off, the observed gradients declined during cooling at night. We assume
371 that the wind blowing across the pond surface drove buoyant cyanobacteria and surface water downwind and
372 caused an upwelling of deeper, colder, and hypoxic water on the upwind side. This wind-related circulation pattern
373 has been described as a “conveyer belt” in classical textbooks (Reynolds et al., 2006), held responsible for a
374 disruption of the thermal structure of the water column and the non-uniform spatial distribution of pH, oxygen,

https://doi.org/10.5194/bg-2023-4
Preprint. Discussion started: 19 January 2023
© Author(s) 2023. CC BY 4.0 License.


CO_2 or CH_4 and also plankton assemblages (e.g. Loken et al., 2019; Natchimuthu et al., 2016; Rinke et al., 2009; Ortiz and Wilkinson, 2021).

Similar to our study, mild winds (~4 m s^{-1}) were strong enough to redistribute heat and induce lake-wide circulations driving upwelling and downwelling in 24 m deep Lake Pleasant (Czikowsky et al., 2018). As the wind blows harder and lasts longer, the effects on ecosystem functioning may target higher trophic levels and become more complex (Rinke et al., 2009). In Lake Constance, a three day storm event with wind velocities of ~10 m s^{-1} resulted in a lake-wide displacement of water masses and the formation of the 6-15 °C horizontal surface water gradient, which in turn changed the spatial distribution of phytoplankton, zooplankton and juvenile fish (Rinke et al., 2009). After several stormy days (wind velocities of 12-15 m s^{-1}), Čech et al. (2011) observed negative effects of wind-driven changes in water temperature and wave action on perch (*Perca fluviatilis*) spawning in the Lake Milada. Although wind events affect shallow and deep lakes differently, there is growing evidence that they can have far-reaching consequences on the functioning of aquatic ecosystems by disrupting energy flows, nutrient fluxes, productivity and reproduction, and consequently altering community composition and trophic interactions in the short and long term (Stockwell et al., 2020). As the frequency, intensity, spatial extent and duration of these extreme meteorological events are projected to increase due to ongoing climate change (Comou and Rahmstorf, 2012), there is an urgent need to better understand the mechanisms underlying their impacts on the maintenance of the ecosystem services.

4.3 Summer changes in the oxygen regime

Our data demonstrate that shallow, hyper-eutrophic ponds have disrupted oxygen regimes (Baxa et al., 2021) with anoxic hypolimnion and may experience severe whole-water column hypoxia critical for aquatic biota (Miranda et al., 2001). The hypoxic periods may result, for example, from sudden weather change (Jeppesen et al., 1990) and last several days, during which physical processes and phytoplankton photosynthesis cannot compensate for intense community respiration (Baxa et al., 2021). This became obvious in August when severe oxygen depletion was measured at the surface across the whole pond, mostly far below a critical level of 4.5 mg L^{-1}, when adverse effects came into play (Banerjee et al., 2019). However, oxygen surface concentrations in shallow parts of the pond were substantially higher regardless of the time of day, which contrasts with findings of Miranda et al. (2001), who emphasised shallow waters as the most sensitive parts of lakes, where hypoxic events can occur due to the respiration of sediment biota. The observed spatial gradients of oxygen may create temporal refugia which allow fish to survive harsh conditions that occur in the deepest part of the pond. To minimise economic losses and negative impacts on the ecosystem, future research should identify the interplay between meteorological forcing,

https://doi.org/10.5194/bg-2023-4
Preprint. Discussion started: 19 January 2023
© Author(s) 2023. CC BY 4.0 License.


trophic status and anthropogenic pressures (e.g. management practices) that affect oxygen fluctuations at various time scales.

4.4 Study limitations

Like in other research, there are some limitations in the current study. Since our measurement had only a limited temporal resolution (three samplings during the summer season), it is not appropriate to extrapolate CH_4 emissions for annual values. Noticeably, future research must increase the frequency of the sampling and include also innovative techniques to measure CH_4 fluxes at multiple fishponds, with different management regime. In our study, the 12 h deployment time of the floating chambers could have led to extensive gas accumulation, which in turn might have resulted in an underestimation of the total CH_4 fluxes due to the dissolution of the CH_4 from the chamber into the water once the equilibrium concentration in the chamber is overcome (Bastviken et al., 2010). However, CH_4 concentrations in water corresponded to a supersaturation of several orders of magnitude, so the introduced bias appears to be of minor importance. In any case, our daily CH_4 fluxes represent a rather conservative estimate for the global methane budget. In our study, we also did not address the important processes that could shed light on the lake CH_4 budget, such as CH_4 oxidation rates (Bastviken et al., 2008) or biological interaction (e.g. protistan grazing on CH_4 oxidising bacteria) in aquatic food webs (Sanseverino et al., 2012) that can affect the overall CH_4 fluxes. We also lack information about spatial differences in sediment microbiota and organic carbon content and compositions, which were found to affect CH_4 production rates (Berberich et al., 2020; Emerson et al., 2021). Despite the limitation mentioned above, our results show that complementary spatial surveys help contextualise the fixed station dynamics and provide additional, management-relevant information about the fishpond.

5. Conclusions

Deciphering the mechanisms that drive spatial and temporal heterogeneity in aquatic ecosystem structure and function not only expands our understanding of pond ecology but also provides insights to improve the management of these ecosystems and the services they provide. Our results suggest that spatial heterogeneity needs to be considered when designing experiments and monitoring programs. Without the spatially resolved sampling, we introduce bias into our datasets, hampering our limnological understanding of the ecosystem's functioning and impeding our ability to accurately estimate rates such as methane emissions on a global scale (DelSontro et al., 2018a). In agreement with Kosten et al. (2020), we demonstrated that neglecting ebullition leads to a considerable underestimating of the total CH_4 fluxes. Since there are thousands of these intensively managed fishponds, we

© Author(s) 2023. CC BY 4.0 License.


argue for changing the management practices toward sustainable use of natural resources to mitigate the overall emissions of greenhouse gases from these ecosystems. Future studies are needed to characterise CH_4 fluxes over a greater number and diversity of aquaculture ponds and examine the mechanisms controlling CH_4 emissions in aquatic ecosystems.

Acknowledgements

The study was supported by the Czech Science Foundation (Research Projects No. 17-09310S, 19-23261S and P504/19-16554S). We thank Dr. Martin Rulík for providing us gas chambers. We especially thank to Prof. Miloslav Šimek and Linda Jíšová for enabling gas analyses. We are grateful Anna Sieczko for consultation on the calculation of CH_4 fluxes. English correction was made by Anton Baer.

Data availability

Dataset associated with the manuscript can be found in the GitHub Repositories under https://zenodo.org/badge/latestdoi/587640213.

Author contributions

All authors contributed to the study conception and design. PZ planned the campaign; PZ, AM and JN performed the sampling and analyzed the data; AM performed the gas-measurements; VK performed statistical analyses and modelling; PZ and AM wrote the manuscript. All authors read and approved the final manuscript.

References

Aben, R.C.H., Barros, N., van Donk, E., Frenken, T., Hilt, S., Kazanjian, G., Lamers, L.P.M., Peeters, E.T.H.M., Roelofs, J.G. M, de Senerpont Domis, L.N., Stephan, S., Velthuis, M., Van de Waal, D.B., Wik, M., Thornton, B.F., Wilkinson, J., DelSontro, T., and Kosten, S.: Cross continental increase in methane ebullition under climate change. Nat. Commun., 8, 1682, https://doi.org/10.1038/s41467-017-01535-y, 2017.

Banerjee, A., Chakrabarty, M., Rakshit, N., Bhowmick, A.R., and Ray, S.: Environmental factors as indicators of dissolved oxygen concentration and zooplankton abundance: deep learning versus traditional regression approach. Ecol. Indic., 100, 99-117, https://doi.org/10.1016/j.ecolind.2018.09.051, 2019.

Baron, A.A.P., Dyck, L.T., Amjad, H., Bragg, J., Kroft, E., Newson, J., Oleson, K., Casson, N.J., North, R.L., Venkiteswaran, J.J., and Whitfield, C.J.: Differences in ebullitive methane release from small, shallow ponds present challenges for scaling. Sci. Total Environ., 802, 149685, https://doi.org/10.1016/j.scitotenv.2021.149685, 2022.

https://doi.org/10.5194/bg-2023-4
Preprint. Discussion started: 19 January 2023
© Author(s) 2023. CC BY 4.0 License.


462 Bartosiewicz, M., Maranger, R., Przytulska, A., and Laurion, I.: Effects of phytoplankton blooms on fluxes and
463 emissions of greenhouse gases in a eutrophic lake. Water Res., 196, 116985,
464 https://doi.org/10.1016/j.watres.2021.116985, 2021.
465 Bastviken, D., Cole, J., Pace M., and Tranvik, L.: Methane emissions from lakes: Dependence of lake
466 characteristics, two regional assessments, and a global estimate. Global Biogeochem. Cycles, 18, GB4009,
467 https://doi.org/10.1029/2004GB002238, 2004.
468 Bastviken, D., Cole, J.J., Pace, M.L., and Van de Bogert, M.C.: Fates of methane from different lake habitats:
469 connecting whole-lake budgets and CH_4 emissions. J. Geophys. Res. Biogeosci., 113, G02024,
470 https://doi.org/10.1029/2007JG000608, 2008.
471 Bastviken, D., Santoro, A.L., Marotta, H., Pinho, L.Q., Calheiros, D.F., Crill, P., and Enrich-Prast, A.: Methane
472 Emissions from Pantanal, South America, during the Low Water Season: Toward More Comprehensive Sampling.
473 Environ. Sci. Tech., 44, 5450-5455, https:///doi.org/10.1021/es1005048, 2010.
474 Bates, D., Maechler, M., Bolker, B., and Walker, S.: Fitting Linear Mixed-Effects Models Using lme4. J. Stat.
475 Soft., 67, 1-48, https://doi.org/10.18637/jss.v067.i01, 2015.
476 Baxa, M., Musil, M., Kummel, M., Hazlík, O., Tesařová, B., and Pechar, L.: Dissolved oxygen deficits in a shallow
477 eutrophic aquatic ecosystem (fishpond) – Sediment oxygen demand and water column respiration alternately drive
478 the oxygen regime. Sci. Total Environ., 766, 142647, https://doi.org/10.1016/j.scitotenv.2020.142647, 2021.
479 Beaulieu, J.J,, DelSontro, T., and Downing, J.A.: Eutrophication will increase methane emissions from lakes and
480 impoundments during the 21st century. Nat. Commun., 10, 3-7, https://doi.org/10.1038/s41467-019-09100-5,
481 2019.
482 Berberich, M.E., Beaulieu, J.J., Hamilton, T.L., Waldo, S., and Buffam, I.: Spatial variability of sediment methane
483 production and methanogen communities within a eutrophic reservoir: Importance of organic matter source and
484 quantity. Limnol. Oceanogr., 65, 1336-1358, https://doi.org/10.1002/lno.11392, 2020.
485 Bižić, M., Klintzsch, T., Ionescu, D., Hindiyeh, M.Y., Günthel, M., Muro-Pastor, A.M., Eckert, W., Urich, T.,
486 Keppler, F., and Grossart, H.P.: Aquatic and terrestrial cyanobacteria produce methane. Sci. Adv., 6, 1-10,
487 https://doi.org/10.1126/sciadv.aax5343, 2020.
488 Bussmann, I., Matoušů, A., Osudar, R., and Mau, S.: Assessment of the radio ^{3}H-CH_4 tracer technique to measure
489 aerobic methane oxidation in the water column. Limnol. Oceanogr.- Meth., 13, 312-327,
490 https://doi.org/10.1002/lom3.10027, 2015.
491 Casper, P., Maberly, S.C., Hall, G.H., and Finlay, B.J.: Fluxes of methane and carbon dioxide from a small
492 productive lake to the atmosphere. Biogeochemistry, 49, 1-19, https://doi.org/10.1023/A:1006269900174, 2000.
493 Čech, M., Peterka, J., Říha, M., Muška, M., Hejzlar, J., and Kubečka, J.: Location and timing of the deposition of
494 eggs strands by perch (*Perca fluviatilis* L.): the roles of lake hydrology, spawning substrate and female size.
495 Knowl. Manag. Aquat. Ecosyst., 403, 1-12, https://doi.org/10.1051/kmae/2011070, 2011.
496 Céréghino, R., Biggs, J., Oertli, B., and Declerck, S.: The ecology of European ponds: defining the characteristics
497 of a neglected freshwater habitat. Hydrobiologia, 597, 1-6, https://doi.org/10.1007/s10750-007-9225-8, 2008.
498 Coumou, D. and Rahmstorf, S.: A decade of weather extreme. Nat. Clim. Change, 2, 491-96,
499 https://doi.org/10.1038/nclimate1452, 2012.
500 Crusius, J. an Wanninkhof, R.: Gas transfer velocities measured at low wind speed over a lake. Limnol. Oceanogr.,
501 48, 1010-1017, https://doi.org/10.4319/lo.2003.48.3.1010, 2003.

© Author(s) 2023. CC BY 4.0 License.

Czikowsky, M.J., MacIntyre, S., Tedford, E.W., Vidal, J., and Miller, S.D.: Effects of wind and buoyancy on carbon dioxide distribution and air-water flux of a stratified temperate lake. J. Geophys. Res. Biogeosci., 123, 2305-2322, https://doi.org/10.1029/2017JG004209, 2018.

De Meester, L., Declerck, S., Stoks, R., Louette, G., Van de Meutter, F., De Bie, T., Michels, E., and Brendonck, L.: Ponds and pools as model systems in conservation biology, ecology and evolutionary biology. Aquat. Cons., 15, 715-725, https://doi.org/10.1002/aqc.748, 2005.

DelSontro, T., Boutet, L., St-Pierre, A., del Giorgio, P.A., and Prairie, Y.T.: Methane ebullition and diffusion from northern ponds and lakes regulated by the interaction between temperature and system productivity. Limnol. Oceanogr., 61, 62-77, https://doi.org/10.1002/lno.10335, 2016.

DelSontro, T., Beaulieu, J.J., and Downing, J.J.: Greenhouse gas emissions from lakes and impoundments: upscaling in the face of global change. Limnol. Oceanogr. Lett., 3, 64-75, https://doi.org/10.1002/lol2.10073, 2018a.

DelSontro, T., del Giorgio, P.A., and Prairie, Y.T.: No Longer a Paradox: The Interaction Between Physical Transport and Biological Processes Explains the Spatial Distribution of Surface Water Methane Within and Across Lakes. Ecosystems, 21, 1073-1087, 10.1007/s10021-017-0205-1, 2018b.

Emerson, J.B., Varner, R.K., Wik, M., Parks, D.H., Neumann, R.B., Johnson, J.E., Singleton, C. M., Woodcroft, B.J., Tollerson II, R., Owusu-Dommey, A., Binder, M., Freitas, N. L., Crill, P.M., Saleska, S.R., Tyson, G.W., and Rich, V.I.: Diverse sediment microbiota shape methane emission temperature sensitivity in Arctic lakes. Nat. Commun., 12, 5815, https://doi.org/10.1038/s41467-021-25983-9, 2021.

Grasset, Ch., Mendonça, R,., Saucedo, G.V., Bastviken, D., Roland, F., and Sobek, S.: Large but variable methane production in anoxic freshwater sediment upon addition of allochthonous and autochthonous organic matter. Limnol. Oceanogr., 63, 1488-1501, https://doi.org/10.1002/lno.10786, 2018.

Halekoh, H. and Hojsgaard, S.: A Kenward-Roger Approximation and Parametric Bootstrap Methods for Tests in Linear Mixed Models - The R Package pbkrtest. J. Stat. Soft., 59, 1-30, https://doi.org/10.18637/jss.v059.i09 2014.

Hofmann, H., Federwisch, L., and Peeters, F.: Wave-induced release of methane: littoral zones as a source of methane in lakes. Limnol. Oceanogr., 55, 1990-2000, https://doi.org/10.4319/lo.2010.55.5.1990, 2010.

Hofmann, H.: Spatiotemporal distribution patterns of dissolved methane in lakes: How accurate are the current estimations of the diffusive flux path? Geophys. Res. Lett., 40, 2779-2784, https://doi.org/10.1002/grl.50453, 2013.

Hu, Z., Wu, S., Ji, Ch., Zou, J., Zhou, Q., and Liu, S.: A comparison of methane emissions following rice paddies conversion to crab-fish farming wetlands in southeast China. Environ. Sci. Pollut. Res., 23, 1505-1515, https://doi.org/10.1007/s11356-015-5383-9, 2016.

Jansen, J., Thornton, B.F., Jammet, M.M., Wik, M., Cortés, A., Friborg, T., MacIntyre, S., and Crill, P.M.: Climate-sensitive controls on large spring emissions of CH_4 and CO_2 from northern lakes. J. Geophys. Res., Biogeosciences, 124, 2379-2399, https://doi.org/10.1029/2019JG005094, 2019.

Jeppesen, E., Søndergaard, M., Sortkjaer, O., Mortensen, E., and Kristensen, P.: Interactions between phytoplankton zooplankton and fish in a shallow hypertrophic Lake a study of phytoplankton collapses in Lake Sobygaard, Denmark. Hydrobiologia, 1991, 149-164, https://doi.org/10.1007/BF00026049, 1990.

Kolar, V., Vlašánek, P., and Boukal, D.S.: The influence of successional stage on local odonate communities in man-made standing waters. Ecol. Eng., 173, 106440, https://doi.org/10.1016/j.ecoleng.2021.106440, 2021.

https://doi.org/10.5194/bg-2023-4
Preprint. Discussion started: 19 January 2023
© Author(s) 2023. CC BY 4.0 License.

542 Kopáček, J. and Hejzlar, J.: Semi-micro determination of total phosphorus in fresh waters with perchloric acid
543 digestion. Int. J. Environ. Anal. Chem., 53, 173-183, https://doi.org/10.1080/03067319308045987, 1993.
544 Kopáček, J. and Procházková, L.: Semi-Micro Determination of Ammonia in Water by the Rubazoic Acid Method.
545 Int. J. Environ. Anal. Chem., 53, 243-248, https://doi.org/10.1080/03067319308045993, 1993.
546 Kosten, S., Almeida, R.M., Barbosa, I., Mendonça, R., Muzitano, I.S., Oliveira-Junior, E.S., Vroom, R.J.E., Wang,
547 H.J., and Barros, N.: Better assessments of greenhouse gas emissions from global fish ponds needed to adequately
548 evaluate aquaculture footprint. Sci. Total Environ., 748, 141247, https://doi.org/10.1016/j.scitotenv.2020.141247,
549 2020.
550 Laas, A., Noges, P., Koiv, T., and Noges, T.: High-frequency metabolism study in a large and shallow temperate
551 lake reveals seasonal switching between net autotrophy and net heterotrophy. Hydrobiologia, 694, 57-74,
552 https://doi.org/10.1007/s10750-012-1131-z, 2012.
553 Loken, L.C., Crawford, J.T., Schramm, P.J., Stadler, P., Desai, A.R., and Stanley, E.H.: Large spatial and temporal
554 variability of carbon dioxide and methane in a eutrophic lake. J. Geophys. Res. Biogeosci., 124, 2248-2266
555 https://doi.org/10.1029/2019JG005186, 2019.
556 Lüdecke, D.: "ggeffects: Tidy Data Frames of Marginal Effects from Regression Models." J. Open Source Soft.,
557 3, 772, https://doi: 10.21105/joss.00772, 2018.
558 Lüdecke, D., Makowski, D., and Waggoner, P.: performance: Assessment of Regression Models Performance. R
559 package version 0.4.4. https://CRAN.R-project.org/package=performance, 2020.
560 Ma, Y., Sun, L., Liu, C., Yang, X., Zhou, W., Yang, B., Schwenke, G., and Liu, D.L.: A comparison of methane
561 and nitrous oxide emissions from inland mixed-fish and crab aquaculture ponds. Sci. Total Environ., 637-638,
562 517-523, https://doi.org/10.1016/j.scitotenv.2018.05.040, 2018
563 McAuliffe, C.: Gas Chromatographic determination of solutes by multiple phase equilibrium. Chem. Technol., 1,
564 46-51, 1971.
565 Miranda, L.E., Hargreaves, J.A., and Raborn, S.W.: Predicting and managing risk of unsuitable dissolved oxygen
566 in a eutrophic lake. Hydrobiologia, 457, 177-185, https://doi.org/10.1023/A:1012283603339, 2001.
567 Murphy, J. and Riley, J.P.: A modified single-solution method for the determination of phosphate in natural waters.
568 Anal. Chim. Acta, 27, 31-36, https://doi.org/10.1016/S0003-2670(00)88444-5, 1962.
569 Natchimuthu, S., Sundgren, I., Gålfalk, M., Klemedtsson, L., Crill, P., Danielsson, Å., and Bastviken, D.: Spatio-
570 temporal variability of lake CH_4 fluxes and its influence on annual whole lake emission estimates. Limnol.
571 Oceanogr., 61, 13-26, https://doi.org/10.1002/lno.10222, 2016.
572 Nijman, T.P.A., Lemmens, M., Lurling, M., Kosten, S., Welte, C., and Veraart, A.J.: Phosphorus control and
573 dredging decrease methane emissions from shallow lakes. Sci. Total Environ., 847, 15758,
574 https://doi.org/10.1016/j.scitotenv.2022.157584, 2022.
575 Ortiz, D.A. and Wilkinson, G.M.: Capturing the spatial variability of algal bloom development in a shallow
576 temperate lake. Freshwater Biol., 66, 2064-2075, https://doi.org/10.1111/fwb.13814, 2021.
577 Ostrovsky, I., McGinnis, D.F., Lapidus, L., and Eckert, W.: Quantifying gas ebullition with echosounder: The role
578 of methane transport by bubbles in a medium-sized lake. Limnol. Oceanogr. Meth., 6, 105-118,
579 https://doi.org/10.4319/lom.2008.6.105, 2008.
580 Pechar, L.: Impacts of long-term changes in fishery management on the trophic level and water quality in Czech
581 fishponds. Fisheries Manag. Ecol., 7, 23-32, 10.1046/j.1365-2400.2000.00193.x, 2000.

© Author(s) 2023. CC BY 4.0 License.


582 Pokorný, J. and Hauser, V.: The restoration of fish ponds in agricultural landscapes. Ecol. Eng., 18, 555-574,
583 https://doi.org/10.1016/S0925-8574(02)00020-4, 2002.
584 Potužák, J., Hůda, J., and Pechar, L.: Changes in fish production effectivity in eutrophic fishponds – impact of
585 zooplankton structure. Aquacult. Int., 15, 201-210, https://doi.org/10.1007/s10499-007-9085-2, 2007.
586 Potužák, J., Duras, J., and Drozd, B.: Mass balance of fishponds: are they sources or sinks of phosphorus?
587 Aquacult. Int., 24, 1725-1745, https://doi.org/10.1007/s10499-016-0071-4, 2016.
588 Prairie, Y.T. and del Giorgio, P.A.: A new pathway of freshwater methane emissions and the putative importance
589 of microbubbles. Inland Waters, 3, 311-320, https://doi.org/10.5268/IW-3.3.542, 2013.
590 Procházková, L.: Bestimmung der Nitrate im Wasser. Zeitschrit für Analytische Chemie, 167, 254-260, 1959.
591 Rasilo, T., Prairie, Y.T., and del Giorgio, P.A.: Large-scale patterns in summer diffusive CH_4 fluxes across boreal
592 lakes, and contribution to diffusive C emissions. Glob. Change Biol., 21, 1124-1139,
593 https://doi.org/10.1111/gcb.12741, 2015.
594 R Core Team: A language and environment for statistical computing. R Foundation for Statistical Computing.
595 Vienna, Austria https://www.R-project.org/, 2018.
596 Reynolds, C.S.: Ecology of phytoplankton, Cambridge University Press, Cambridge,
597 https://doi.org/10.1017/CBO9780511542145, 2006.
598 Rinke, K., Huber, A.M.R., Kempke, S., Eder, M., Wolf, T., Probst, W.N., and Rothhaupt, K.: Lake-wide
599 distributions of temperature, phytoplankton, zooplankton, and fish in the pelagic zone of a large lake. Limnol.
600 Oceanogr., 54, 1306-1322, https://doi.org/10.4319/lo.2009.54.4.1306, 2009.
601 Rutegwa, M., Potužák, J., Hejzlar, J., and Drozd, B.: Carbon metabolism and nutrient balance in a hypereutrophic
602 semi-intensive fishpond. Knowl.Manag. Aquat. Ecosyst., 49, https://doi.org/10.1051/kmae/2019043, 2019.
603 Sanseverino, A.M., Bastviken, D., Sundh, I., Pickova, J., and Enrich-Prast, A.: Methane carbon supports aquatic
604 food webs to the fish level. PLoS One7, e42723, https://doi.org/10.1371/journal.pone.0042723, 2012.
605 Scheffer, M.: Ecology of shallow lakes. Population and Community Biology Series. Springer, 357 p.,
606 https://doi.org/10.1007/978-1-4020-3154-0, 2004.
607 Schilder, J., Bastviken, D., van Hardenbroek, M., Kankaala, P., Rinta, P., Stötter, T., and Heiri, O.: Spatial
608 heterogeneity and lake morphology affect diffusive greenhouse gas emission estimates of lakes. Geophys. Res.
609 Lett., 40, 5752-5756, https://doi.org/10.1002/2013GL057669, 2013.
610 Schmiedeskamp, M., Praetzel, L.S.E., Bastviken, D., and Knorr, K.H.: Whole-lake methane emissions from two
611 temperate shallow lakes with fluctuating water levels: Relevance of spatiotemporal patterns. Limnol. Oceanogr.,
612 66, 2455-2469, https://doi.org/10.1002/lno.11764, 2021.
613 Stanley, E.H., Collins, S.M., Lottig, N.R., Oliver, S.K., Webster, K.E., Cheruvelil, K.S., and Soranno, P.A.: Biases
614 in lake water quality sampling and implications for macroscale research. Limnol. Oceanogr., 64, 1572-1585,
615 https://doi.org/10.1002/lno.11136, 2019.
616 Stockwell, J.D., Doubek, J.P., Adrian, R., Anneville, O., Carey, C.C., Carvalho, L., Domis, L.N.D.S., Dur, G.,
617 Frassl, M.A., Grossart, H.-P., Ibelings, B.W., Lajeunesse, M.J., Lewandowska, A.M., Llames, M.E., Matsuzaki,
618 S.-I.S., Nodine, E.R., Nõges, P., Patil, V.P., Pomati, F., Rinke, K., Rudstam, L.G., Rusak, J.A., Salmaso, N.,
619 Seltmann, C.T., Straile, D., Thackeray, S.J., Thiery, W., Urrutia-Cordero, P., Venail, P., Verburg, P., Woolway,
620 R.I., Zohary, T., Andersen, M.R., Bhattacharya, R., Hejzlar, J., Janatian, N., Kpodonu, A.T.N.K., Williamson,

© Author(s) 2023. CC BY 4.0 License.

T.J., and Wilson, H.L.: Storm impacts on phytoplankton community dynamics in lakes. Glob. Change Biol., 26, 2756-2784, https://doi.org/10.1111/gcb.15033, 2020.

Tranvik, L.J., Downing, J.A., Cotner, J.B., Loiselle, S.A., Striegl, R.G., Ballatore, T.J., Dillon, P., Finlay, K., Fortino, K., Knoll, L.B., Kortelainen, P.L., Kutser, T., Larsen, S., Laurion, I., Leech, D.M., McCallister, S.L., McKnight, D.M., Melack, J.M., Overholt, E., Porter, J.A., Prairie, Y.T., Renwick, W.H., Roland, F., Sherman, B.S., Schindler, D.W., Sobek, S., Tremblay, A., Vanni, M.J., Verschoor, A.M., von Wachenfeldt, E., Weyhenmeyer, G.A.: Lakes and reservoirs as regulators of carbon cycling and climate. Limnol. Oceanogr., 54, 2298-2314, https://doi.org/10.4319/lo.2009.54.6_part_2.2298, 2009.

van Bergen, T.J.H.M., Barros, N., Mendonça, R., Aben, R.C.H., Althuizen, I.H.J., Huszar, V.,Lamers, L.P.M., Lürling, M., Roland, F., Kosten, S.: Seasonal and diel variation in greenhouse gas emissions from an urban pond and its major drivers. Limnol. Oceanog., 64, 2129-2139, https://doi.org/10.1002/lno.11173, 2019.

Varadharajan, Ch. and Hemond, H.F.: Time-series analysis of high-resolution ebullition fluxes from a stratified, freshwater lake. J. Geophys. Res., 117, G02004, https://doi.org/10.1029/2011JG001866, 2012.

Wanninkhof, R.: Relationship between wind speed and gas exchange over the ocean revisited. Limnol. Oceanogr. Methods, 12, 351-362, https://doi.org/10.4319/lom.2014.12.351, 2014.

Wiesenburg, D.A. and Guinasso N.L.: Equilibrium solubilities of methane, carbon monoxide, and hydrogen in water and sea water. J. Chem. Eng. Data, 24, 356-360, https://doi.org/10.1021/je60083a006, 1979.

Wik, M., Varner, R.K., Anthony, K.W., MacIntyre, S., and Bastviken, D.: Climate-sensitive northern lakes and ponds are critical components of methane release. Nat. Geosci., 9, 99-105, https://doi.org/10.1038/ngeo2578, 2016.

Xiao, Q., Zhang, M., Hu, Z., Gao, Y., Hu, Ch., Liu, Ch., Liu, S., Zhang, Z., Zhao, J., Xiao, W., and Lee, X.: Spatial variations of methane emission in a large shallow eutrophic lake in subtropical climate. J. Geophys. Res. Biogeosci., 122, https://doi.org/10.1002/2017JG003805, 2017.

Yamamoto, S., Alcauskas, J.B., and Crozier, T.E. Solubility of methane in distilled water and seawater. J. Chem. Eng. Data, 21, 78-80, https://doi.org/10.1021/je60068a029, 1976.

Yan, X., Xu, X., Ji, M., Zhang, Z., Wang, M., Wu, S., Wang, G., Zhang, Ch., and Liu, H.: Cyanobacteria blooms: A neglected facilitator of CH_4 production in eutrophic lakes. Sci. Total Environ., 651, 466-474, https://doi.org/10.1016/j.scitotenv.2018.09.197, 2019.

Yang, P., Zhang, Y., Yang, H., Zhang, Y., Xu, J., Tan, L., Tong, C., and Lai, D.Y.: Large fine-scale spatiotemporal variations of CH_4 diffusive fluxes from shrimp aquaculture ponds affected by organic matter supply and aeration in Southeast China. J. Geophys. Res. Biogeosci., 124, 1290-1307, https://doi.org/10.1029/2019JG005025, 2019.

Yang, P., Zhang, Y., Yang, H., Guo, Q., Lai, D.Y.F., Zhao, G., Li, L., and Tong, C.: Ebullition was a major pathway of methane emissions from the aquaculture ponds in Southeast China. Water Res., 184, 116176, https://doi.org/10.1016/j.watres.2020.116176, 2020.

Yuan, J., Xiang, J., Liu, D.Y., Kang, H., He, T.H., Kim, S., Lin, Y.X., Freeman, C., and Ding, W.X.: Rapid growth in greenhouse gas emissions from the adoption of industrial-scale aquaculture. Nat. Clim. Chang., 9, 318-322, https://doi.org/10.1038/s41558-019-0425-9, 2019.

Yuan, J., Liu, D., Xiang, J., He, T., Kang, H., and Ding, W.: Methane and nitrous oxide have separated production zones and distinct emission pathways in freshwater aquaculture ponds. Water Research, 190, 116739, https://doi.org/10.1016/j.watres.2020.116739, 2021.

https://doi.org/10.5194/bg-2023-4
Preprint. Discussion started: 19 January 2023
© Author(s) 2023. CC BY 4.0 License.

661 Zar, J.H.: Biostatistical analysis. Prentice Hall, Inc., Englewood Cliffs, New York, 663 p., 1984.
662 Zhang, L., Liao, Q., Gao, R., Luo, R., Liu, Ch., Zhong, J., and Wang, Z.: Spatial variations in diffusive methane
663 fluxes and the role of eutrophication in a subtropical shallow lake. Sci. Total Environ., 759, 143495,
664 https://doi.org/10.1016/j.scitotenv.2020.143495, 2021.
665 Zhao, J., Zhang, M., Xiao, W., Jia, L., Zhang, X., Wang, J., Zhang, Z., Xie, Y., Yini Pu, Liu, S., Feng, Z., Lee X.:
666 Large methane emission from freshwater aquaculture ponds revealed by long-term eddy covariance observation.
667 Agric. For. Meteorol., 308-309, 108600, https://doi.org/10.1016/j.agrformet.2021.108600, 2021.
668 Zhou, Y.Q., Zhou, L., Zhang, Y.L., de Souza, J.G., Podgorski, D.C., Spencer, R.G.M., Jeppesen, E., and Davidson,
669 T.A.: Autochthonous dissolved organic matter potentially fuels methane ebullition from experimental lakes. Water
670 Res., 166, 115048, https://doi.org/10.1016/j.watres.2019.115048, 2019.
671 Zuur, A.F., Ieno, E.N., Walker, N.J., Saveliev, A.A., and Smith, G.M.: Mixed effects models and extensions in
672 ecology with R. Springer, New York, USA, 574 p, https://doi.org/10.1007/978-0-387-87458-6, 2009.
673